Molecular Recognition in Acetylcholinesterase Catalysis: Free-Energy Correlations for Substrate Turnover and Inhibition by Trifluoro Ketone Transition-State Analogs[†,‡]

Haridasan K. Nair, Javier Seravalli, Tomira Arbuckle, and Daniel M. Quinn*

Department of Chemistry, University of Iowa, Iowa City, Iowa 52242

Received January 21, 1994; Revised Manuscript Received April 28, 1994[⊗]

ABSTRACT: Ten *meta*-substituted aryl trifluoromethyl ketones (*m*-$XC_6H_4COCF_3$; X = H, CH_3, CF_3, C_2H_5, isopropyl, *t*-butyl, NH_2, NMe_2, N^+Me_3, NO_2) have been evaluated as inhibitors of acetylcholinesterases from *Electrophorus electricus* and *Torpedo californica*. Trifluoro ketones that have small *meta* substituents (X = H, CH_3, CF_3, C_2H_5, NH_2, NO_2) are rapid reversible inhibitors, whereas the remaining compounds in this study show time-dependent inhibition. Dissociation constants (K_i values) for these compounds span a range of $\sim 10^7$-fold, with trifluoroacetophenone (X = H) being the least potent and *m*-(*N*,*N*,*N*-trimethylammonio)trifluoroacetophenone (X = Me_3N^+) being the most potent inhibitor. For the latter compound K_i values are 1.5 and 15 fM for inhibitions of the respective acetylcholinesterases (Nair, H. K., Lee, K., & Quinn, D. M. (1993) *J. Am. Chem. Soc. 115*, 9939–9941). Linear correlations of $\log(k_{cat}/K_m)$ for substrate turnover versus pK_i of inhibitors have slopes of ~ 0.6, which suggest that aryl trifluoro ketones bind to AChE in a manner that structurally resembles transition states in the acylation stage of catalysis. Substituent variation in the inhibitors allows one to gauge the importance for AChE function of molecular recognition in the quaternary ammonium binding locus of the active site. This locus is frequently termed the "anionic site" and consists of E199, W84, and perhaps Y130 and F330. Correlations of pK_i versus hydrophobicity constant are linear for alkyl and trifluoromethyl substituents but fail for nitrogen-containing substituents. However, three-dimensional correlations of pK_i versus σ_m and molar refractivity of substituents indicate that dispersion interactions in the anionic locus contribute $\sim 10^5$-fold ($\Delta\Delta G$ = 7 kcal mol^{-1}) to the above-mentioned 10^7-fold range of inhibitor potencies. The remaining ~ 100-fold arises from the inductive electronic effects of substituents on the stability of the tetrahedral adduct that forms between the ketone carbonyl of inhibitors and S200 in the esteratic locus of the active site. Values of k_{on}, the second-order rate constant for binding of time-dependent inhibitors, monitor a diffusion-controlled process. Moreover, k_{on} for the quaternary ammonio inhibitor is 20–70-fold higher than for inhibitors that have uncharged *meta* substituents, which likely reflects the effect of the electrical field of AChE on ligand and substrate binding.

The primacy of transition-state stabilization as a source of enzyme catalytic power has long been appreciated (Pauling, 1948; Schowen, 1978; Fersht, 1974). An accounting of transition-state stabilization can be had by answering three questions: What functional groups (i.e., amino acid side chains, solvent molecules, cofactors, other ligands) are involved in molecular recognition of the substrate in the transition state? What roles do these groups play? What quantitative contributions do they make to catalysis?

Acetylcholinesterase (AChE)[1] catalyzes the hydrolysis of the neurotransmitter ACh, a task which the enzyme effects with very high efficiency (Quinn, 1987; Rosenberry, 1975; Schowen, 1978). Recently reported crystal structures of TC-AChE complexes (Sussman *et al.*, 1991; Harel *et al.*, 1993) provide templates for speculation on the roles of active site residues in molecular recognition of the transition state. In the complex with edrophonium the quaternary ammonio function of the ligand is interacting with the aromatic side chains of W84[2] and F330, while modeling of the tetrahedral intermediates in ACh (Sussman *et al.*, 1991) and ATCh (Selwood *et al.*, 1993) hydrolyses indicates additional interactions with E199 and Y130. Hence, the overall picture is that the side chains of E199, F330, W84, and Y130 contribute to the "anionic site" which interacts with the quaternary ammonium pole of ACh in physiological AChE catalysis. Controversy continues on the roles played by these residues. Early on, Wilson and colleagues speculated that an ion pair forms between ACh and an anionic amino acid side chain (Froede & Wilson, 1971), a role that E199 could play. Cohen and colleagues studied the effects of structural variation of substrates on reactivity and of inhibitors on affinity (Hasan *et al.*, 1980, 1981) and consequently suggested that there is no anionic site. In particular, they found that substrate reactivity correlated well with the partial molal volume of the alcohol leaving group, which they claim is consistent with a hydrophobic trimethyl binding site.

[†] Supported by NIH Grants NS21334 to D.M.Q. and GM18360 to P.T. T.A. was supported by an NSF-REU Summer Undergraduate Research Fellowship, Grant CHE 93-0047.

[‡] A portion of this work was conducted in the laboratories of Professor Palmer Taylor while D.M.Q. was a Visiting Professor in the Department of Pharmacology at the University of California—San Diego.

* To whom correspondence should be addressed.

[⊗] Abstract published in *Advance ACS Abstracts,* June 15, 1994.

[1] Abbreviations: ACh, acetylcholine; AChE, acetylcholinesterase; ATCh, acetylthiocholine; DTNB, 5,5′-dithiobis(2-nitrobenzoic acid); EE-AChE, *Electrophorus electricus* AChE; FTIR, Fourier transform infrared; GC/MS, gas chromatography/mass spectroscopy; HPLC, high-performance liquid chromatography; MR, molar refractivity; NMR, nuclear magnetic resonance; PNP, *p*-nitrophenol; PNP^-, *p*-nitrophenoxide anion; ppm, parts per million; TC-AChE, *Torpedo californica* AChE; TMS, tetramethylsilane; UV, ultraviolet. Single-letter amino acid codes: A, alanine; E, glutamate; F, phenylalanine; S, serine; W, tryptophan; Y, tyrosine.

[2] The amino acid sequence numbering used throughout this paper is that of *Torpedo californica* AChE.

0006-2960/94/0433-8566$04.50/0

Chart 1: Trifluoro Ketone Inhibitors and Substrates of AChE

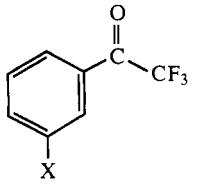

X = H, **1**; Me, **2**; Et, **3**; iPr, **4**; tBu, **5**; CF_3, **6**; NH_2, **7**; NMe_2, **8**; $^+NMe_3$, **9**; NO_2, **10**

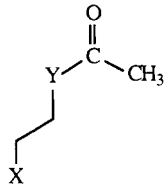

Y = O; X = H, Me, Et, iPr, tBu, NHMe, NMe_2, $^+NMe_3$

Y = S; X = H, NMe_2, $^+NMe_3$

Site-directed mutagenesis experiments may shed some light on the roles of E199 and W84. Values of k_{cat}/K_m for the E199Q mutant of TC-AChE and the W84A mutant of human AChE are reduced 50-fold (Radic *et al.*, 1992) and 3000-fold (Ordentlich *et al.*, 1993), respectively, when compared to the corresponding wild-type enzymes. Because of the large effect of the W84A change, Ordentlich *et al.* claim that W84 is the anionic site that interacts with the quaternary ammonium pole of ACh. The smaller though important effect of the E199Q change suggests that E199 interacts electrostatically with the quaternary ammonium pole of ACh.

The importance of carboxylate residues in AChE function is virtually undeniable. Nolte *et al.* (1980), working with EE-AChE, characterized the ionic strength dependences of k_{cat}/K_m for ATCh hydrolysis and of the rate constant for *N*-methylacridinium binding. They suggested that multiple anionic residues are important for catalysis and ligand binding. Their interpretations are supported by theoretical descriptions of the role of electrostatics in AChE function (Tan *et al.*, 1993; Ripoll *et al.*, 1993). Because AChE has an isoelectric point of 5.5, the molecule possesses a net negative charge at neutral pH. However, there are preponderances of negative and positive residues on opposite halves of the molecule, such that AChE has a quadrupolar electrical field whose dipole moment is oriented along the active site gorge. The positive charge of the substrate, ACh, is attracted to the gorge opening by the negative component of the quadrupolar field and is probably stabilized in the active site by interaction with this field.

In this paper we describe the interactions of *meta*-substituted aryl trifluoromethyl ketones (cf. Chart 1) with EE-AChE and TC-AChE. Moreover, kinetic parameters for AChE-catalyzed turnover of variously substituted acetate ester substrates (cf. Chart 1) have been determined. Systematic variation of substituent structure allows the formulation of free-energy correlations which reveal the nature of molecular interactions between inhibitors and the anionic site of AChE. As we shall see, these correlations contrast with certain ideas that have arisen in the recent literature concerning the role of anionic site residues in AChE catalysis. Moreover, a quantitative accounting is rendered of dispersion interactions and electronic effects that provide a substantial fraction of the catalytic acceleration that AChE brings to bear on ACh hydrolysis.

MATERIALS AND METHODS

Materials. Trifluoroacetophenone, compound **1** in Chart 1; 2-(dimethylamino)ethanol; 2-(methylamino)ethanol; 2-(dimethylamino)ethanethiol·HCl; propyl acetate; butyl acetate; isoamyl acetate; and 3,3-dimethyl-1-butanol were purchased from Aldrich Chemical Co. Acetic anhydride and HPLC grade ethyl acetate were purchased from EM Science, and ethyl thioacetate was from MTM Research Chemicals. ATCh iodide, ACh iodide, DTNB, and *p*-nitrophenol were purchased from Sigma Chemical Co. EE-AChE, type V-S, was purchased from Sigma and before use was dissolved in 0.1 M sodium phosphate buffer, pH 7.3, that contained sufficient NaCl so that the ionic strength was 0.32. Samples of this enzyme that were purified by affinity chromatography on tacrine–Sepharose (Carroll & Emmerling, 1991) gave kinetic parameters that were indistinguishable from those of the commercial preparation. TC-AChE was provided *gratis* by Professor Israel Silman of the Weizmann Institute, Rehovot, Israel. AChE concentrations were determined by active site titration with diethylumbelliferyl phosphate (Schlom *et al.*, 1994). Water for buffer preparation was distilled and then deionized by passage through a mixed-bed ion-exchange column (Barnstead, Sybron Corp.). Buffer pH values were measured on a Corning Model 125 pH meter that is equipped with a glass combination electrode.

Synthesis of Inhibitors. Synthesis and characterization of inhibitors **2**–**6** were described by Nair and Quinn (1993), and those of inhibitors **8** and **9**, by Nair *et al.* (1993). Inhibitor **7** was synthesized from **1** by the following procedure. Trifluoroacetophenone was nitrated to give *m*-nitrotrifluoroacetophenone (compound **10**) by the procedure of Stewart and Vander Linden (1960). The reduction of **10** was accomplished by the procedure of Klabunde and Burton (1970). A mixture of **10** (1.3 g, 5.9 mmol), Sn granules (1.2 g, 10 mmol), and concentrated HCl (5 mL) was refluxed in a round-bottomed flask for 1 h. The resultant reaction mixture was neutralized with aqueous $NaHCO_3$ and extracted with 50 mL of CH_2Cl_2. The CH_2Cl_2 phase was washed with 15 mL of water, dried over $MgSO_4$, and concentrated by rotary evaporation. The product, a brownish-yellow viscous liquid, was obtained on freeze-drying at −78 °C at 0.5 mmHg. ^{19}F NMR in $CDCl_3$ showed a singlet at −70.8 ppm; the corresponding literature value is −70.7 ppm (Klabunde & Burton, 1970). Additional spectroscopic characterizations include the following: (a) ^1H NMR in $CDCl_3$: 3.87, broad singlet, 2H, NH_2; 6.88, multiplet, 1H, aromatic proton; 7.27, multiplet, 2H, aromatic protons; 7.42 ppm, multiplet, 1H, aromatic proton. (b) GC/MS, *m*/*z* (% rel intensity): 189 (M^+, 61), 120 (93), 92 (100), 69 (8), 65 (55). (c) FTIR in CCl_4: 1720 cm^{-1} for >C=O.

Synthesis of Substrates. All synthetic manipulations were done with stirring and under an Ar atmosphere. 3,3-Dimethylbutyl acetate (cf. Chart 1; X = *t*Bu, Y = O) was synthesized by adding 2.2 g of 3,3-dimethyl-1-butanol to 20 mL of $CHCl_3$ in a 100-mL round-bottomed flask. To this was added slowly 4.9 g of acetic anhydride, followed by addition of ~0.2 mL of concentrated H_2SO_4, and the reaction mixture was stirred for 24 h. The mixture was extracted successively with 2 × 20 and 10 mL of 1 M Na_2CO_3 and with 2 × 15 mL of distilled water and was dried over $MgSO_4$. After rotary evaporation of the $CHCl_3$ solvent, the product was isolated by fractional distillation under reduced pressure (20 mmHg); 2 g of product (65% yield) was collected at 65 °C. 2-(*N*-Methylamino)ethyl acetate and 2-(*N*,*N*-dimethylamino)ethyl acetate (cf. Chart 1; X = NHMe and NMe_2, respectively; Y = O) were synthesized from 2-(*N*-methylamino)ethanol and 2-(*N*,*N*-dimethylamino)ethanol, respectively, by essentially the same procedure as that above, save that H_2SO_4 was not added to the reaction mixtures. FTIR spectra for the three esters contained the expected carbonyl stretches, and ^1H NMR

spectra were consistent with the structures of the substrates.

Synthesis of 2-(dimethylamino)ethyl thioacetate involved the following manipulations. To 70 mL of 0.6 M aqueous Na_2S was added 7 g (50 mmol) of 2-(dimethylamino)-ethanethiol·HCl, and the mixture was extracted with 3 × 25 mL of $CHCl_3$. The yield of the neutralized and extracted thioalcohol was determined by coupling with DTNB in an aqueous 0.1 M sodium phosphate buffer at pH 7.1. The coupling reaction produces 2-nitro-5-thiobenzoic acid, which absorbs at 412 nm with an absorptivity constant of 13 600. To the $CHCl_3$ extract that contained 26 mmol of 2-(dimethylamino)ethanethiol was slowly added 2.7 g (27 mmol) of acetic anhydride, and the mixture was stirred overnight at room temperature and under an Ar atmosphere. The overnight reaction mixture was extracted with 3 × 10 mL of 1 M aqueous Na_2CO_3, and the combined Na_2CO_3 extracts were washed with 10 mL of $CHCl_3$. The $CHCl_3$ layers were combined, dried over $MgSO_4$, gravity filtered, and rotoevaporated. The residue was fractionally distilled at 20 mmHg, and the product (2.2 g, 65% yield) was isolated as the fraction that boiled at 96 °C. The ^1H NMR spectrum (in $CDCl_3$) contained the following features: 2.33, s, 3H, CH_3CO; 2.26, s, 6H, Me_2N; 2.48, t (J = 7 Hz), 2H; 3.01 ppm, t (J = 7 Hz), 2H, CH_2S and CH_2N.

Spectroscopy. NMR spectra were recorded on a Bruker AC-300 spectrometer. For spectra determined in $CDCl_3$, ^{19}F and ^1H chemical shifts are reported in ppm upfield of internal $CFCl_3$ and downfield of internal TMS, respectively. For spectra determined in H_2O or D_2O, ^{19}F and ^1H chemical shifts are referenced against external $CFCl_3$ and external TMS in $CDCl_3$, respectively. FTIR and GC/MS spectra were recorded on Mattson Cygnus 25 and VG TRIO-1 spectrometers, respectively, the latter operated in the electron impact mode at 70 eV.

Enzyme Kinetics. AChE-catalyzed hydrolyses of thioesters were followed by the Ellman assay (Ellman *et al.*, 1961), in which DTNB is coupled with the thioalcohol product to give 2-nitro-5-thiobenzoic acid, which absorbs at 412 nm. AChE-catalyzed hydrolyses of oxy esters were followed by a coupled indicator assay in dilute *p*-nitrophenol buffers. These reactions were followed at 400 nm as the protons that were produced protonated the base component of the buffer. Reactions were followed on HP8452A UV–visible spectrophotometers and were thermostated to ±0.1 °C by using circulating, refrigerated water baths and a jacketed cell holder.

Michaelis–Menten parameters were determined by fitting initial velocity versus substrate concentration data to the following equation (Wentworth, 1965):

$$v = \frac{V_{max}[S]}{K_m + [S] + [S]^2/K_{ss}} \quad (1)$$

At high concentrations substrate binds to a second site on AChE and substrate inhibition is observed (Vellom *et al.*, 1993); K_{ss} is the dissociation constant for binding to the substrate inhibition site.

Compounds **1–3**, **6**, **7**, and **10** are rapid, reversible inhibitors, and hence their inhibition mechanisms were determined by measuring the initial rate, v, of AChE-catalyzed hydrolysis of ATCh at various substrate concentrations and at different fixed inhibitor concentrations. At each inhibitor concentration the apparent Michaelis–Menten parameters were calculated by nonlinear least-squares fitting (Wentworth, 1965) of initial rates to eq 2:

$$v = \frac{V_{app}[S]}{K_m^{app} + [S]} \quad (2)$$

The highest [S] employed was $\ll K_{ss}$, thus avoiding the complication of substrate inhibition. Lineweaver–Burk plots were constructed from the parameters K_m^{app} and V_{app} of the least-squares analyses. The inhibition constants K_i^E and K_i^{ES} were calculated from replots of V_{app}/K_m^{app} and V_{app}, respectively, versus [I]. The requisite replot equations are given in footnote *d* of Table 2. For these compounds K_i^E values were also determined by fitting initial rate versus inhibitor concentration data, collected at a single substrate concentration, to eq 3 (Wentworth, 1965):

$$v_I = \frac{v_0 K_i^{app}}{K_i^{app} + [I]} \quad (3)$$

In eq 3 v_I and v_0 are initial rates in the presence and absence of inhibitor, respectively, and K_i^{app} is the apparent AChE–inhibitor dissociation constant.

Compounds **4**, **5**, **8**, and **9**, on the other hand, are time-dependent AChE inhibitors. Cha has presented a thorough discussion of the kinetics of tight-binding time-dependent enzyme inhibitors, from which the treatment described herein draws extensively (Cha, 1975). For compounds **4**, **5**, **8**, and **9** the inhibition kinetics were characterized by using continuous and stopped-time assays. In the continuous assay the time course of turnover of ATCh is biphasic and is described by the following equation:

$$A = A_0 + \frac{v_0 - v_{ss}}{k}(1 - e^{-kt}) + v_{ss}t \quad (4)$$

This equation describes a reaction that consists of a nonlinear, first-order phase in which the EI complex is accumulating and a subsequent, linear, steady-state phase, wherein equilibrium binding of the inhibitor to AChE has been realized. A and A_0 are absorbances at times t and 0, respectively; v_{ss} is the slope of the steady-state phase; v_0 is the initial velocity of the inhibition time course; and k is the observed pseudo-first-order rate constant for approach to the linear phase. Inhibition time courses were fit to eq 4 by nonlinear least-squares procedures (Wentworth, 1965) to give values of v_{ss}, v_0, and k. Use of eq 4 requires that substrate depletion is negligible. Hence, control reactions (i.e., no inhibitor added) must be linear over the absorbance range of the inhibition time course.

In the stopped-time assay the AChE activity is determined at various times after addition of inhibitor to the enzyme by removing aliquots from the mixture and measuring initial rates of ATCh hydrolysis. The resulting dependence of activity on time is fit by nonlinear least-squares procedures (Wentworth, 1965) to eq 5:

$$v = (v_0 - v_{ss})e^{-kt} + v_{ss} \quad (5)$$

In this equation v and v_{ss} are rates measured at times t and infinity, respectively; v_0 is the rate of the control reaction (i.e., no inhibitor added); and k is the observed rate constant.

For time-dependent AChE inhibitors, K_i^{app} was determined by fitting data to an equation that is identical *pro forma* to eq 3, albeit one in which v_{ss} is the dependent variable:

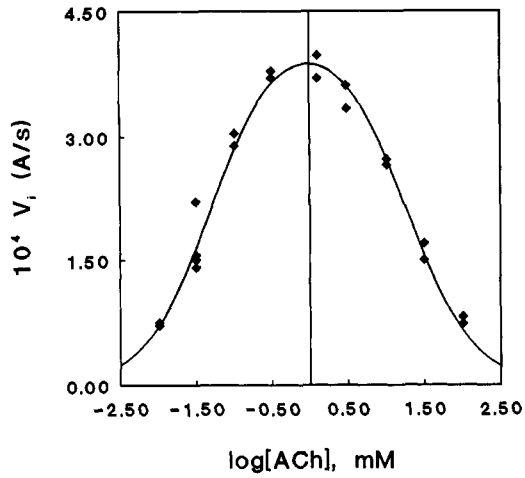

FIGURE 1: Dependence of initial velocities of TC-AChE-catalyzed hydrolysis of ACh on substrate concentration. Reactions were followed at 25.0 ± 0.1 °C by the coupled *p*-nitrophenoxide indicator assay described under Enzyme Kinetics in Materials and Methods. Reaction mixtures contained 0.1 mM PNP/PNP⁻ buffer, pH 7.88, 0.25 M NaCl, 0.045 mM TX100, 24 pM TC-AChE, and the concentrations of ACh that are plotted as logs. The solid line is a nonlinear least-squares fit (Wentworth, 1965) to eq 1; parameters derived from the fit are listed in Table 1.

$$v_{ss} = \frac{v_0 K_i^{app}}{K_i^{app} + [I]} \quad (6)$$

For both rapid, reversible and time-dependent AChE inhibitors, K_i' values were calculated according to eq 7, which accounts for the effect of substrate concentration on K_i^{app}:

$$K_i' = K_i^{app}/(1 + [S]/K_m) \quad (7)$$

K_m is the Michaelis constant measured in the absence of inhibitor.

In aqueous solution the trifluoro ketones are equilibrium mixtures of the free ketone and the ketone hydrate. Hydration equilibrium constants, or K_{hyd} values, were determined by ^{19}F NMR, as described by Nair *et al.* (1993). Since only the free ketones are effective AChE inhibitors (Allen & Abeles, 1989; Brodbeck *et al.*, 1979; Nair *et al.*, 1993), dissociation constants for ketone inhibitors were calculated from K_i' values according to eq 8:

$$K_i^E = K_i'/(K_{hyd} + 1) \quad (8)$$

Molecular Modeling. Models of ACh and m-(*N*,*N*,*N*-trimethylammonio)trifluoroacetophenone were constructed by using the molecular modeling program Sybyl (Tripos Associates, St. Louis, MO). Geometry optimization utilized the molecular mechanics force field of the Sybyl program.

RESULTS

Figure 1 shows that initial velocities of TC-AChE-catalyzed hydrolysis of ACh are subject to marked substrate inhibition at high concentration. Kinetic and substrate inhibition constants for this and the other substrates in Chart 1 were obtained by fitting data to eq 1 and are gathered in Table 1.

Trifluoro ketones that contain *meta* substituents H, Me, Et, CF_3, NH_2, and NO_2 are rapid, reversible inhibitors of both EE-AChE and TC-AChE, as shown in Figure 2 for compound **3**. The pattern of Lineweaver–Burk plots in this figure is consistent with a mixed inhibition mechanism (Segel, 1975) in which the inhibitor binds to the free enzyme and to ES complexes, with respective dissociation constants K_i^E and K_i^{ES}. K_i values for these rapid inhibitors are given, along with other data, in Table 2.

On the other hand, trifluoro ketones that contain the *meta* substituents *i*Pr, *t*Bu, Me_2N, and Me_3N^+ are time-dependent inhibitors of both enzymes, as shown in Figure 3A for compound **4**. For time-dependent AChE inhibitors, the first-order rate constant for approach to equilibrium inhibition was determined as a function of [I]. As shown in Figure 3B, the resulting plots are linear (**8** is an exception; see below),

Table 1: Rate and Substrate Inhibition Constants for AChE-Catalyzed Hydrolyses of Acetate Esters[a]

substrate[b]	enzyme	k_{cat}, s^{-1}	k_{cat}/K_m, M^{-1} s^{-1}	K_{ss}, mM
Y = O, X = H	EE-AChE	*c*	(3.4 ± 0.2) × 10^3	*c*
	TC-AChE	*c*	(2.1 ± 0.1) × 10^3	*c*
Y = S, X = H	TC-AChE	490 ± 30	(1.4 ± 0.2) × 10^4	*c*
Y = O, X = Me	EE-AChE	1400 ± 100	(2.1 ± 0.5) × 10^4	*c*
	TC-AChE	900 ± 200	(1.4 ± 0.6) × 10^4	*c*
Y = O, X = Et	EE-AChE	1650 ± 50	(1.03 ± 0.06) × 10^5	*c*
	TC-AChE	1700 ± 80	(1.2 ± 0.1) × 10^5	*c*
Y = O, X = *i*Pr	EE-AChE	8000 ± 300	(4.5 ± 0.6) × 10^6	*c*
	TC-AChE	3200 ± 100	(1.5 ± 0.2) × 10^6	*c*
Y = O, X = *t*Bu	EE-AChE	2240 ± 60	(2.7 ± 0.3) × 10^6	*c*
	TC-AChE	1980 ± 70	(7 ± 1) × 10^6	240 ± 60
Y = O, X = NHMe	EE-AChE	108 ± 2	(1.44 ± 0.09) × 10^5	120 ± 10
	TC-AChE	147 ± 6	(1.1 ± 0.1) × 10^5	70 ± 10
Y = O, X = NMe_2	EE-AChE	5200 ± 700	(6 ± 1) × 10^6	2.0 ± 0.4
	TC-AChE	1400 ± 200	(2.8 ± 0.4) × 10^6	4.1 ± 0.9
Y = S, X = NMe_2	EE-AChE	14 000 ± 2000	(8 ± 2) × 10^6	3.7 ± 0.8
	TC-AChE	980 ± 40	(6.1 ± 0.7) × 10^6	46 ± 8
Y = O, X = N^+Me_3	EE-AChE	10 400 ± 300	(5.4 ± 0.6) × 10^7	28 ± 3
	TC-AChE	2600 ± 200	(4.9 ± 0.7) × 10^7	19 ± 3
	TC-AChE[d]	5000 ± 500	(1.7 ± 0.3) × 10^8	*e*
Y = S, X = N^+Me_3	EE-AChE	8100 ± 200	(5.0 ± 0.4) × 10^7	33 ± 3
	TC-AChE	6000 ± 2000	(1.6 ± 0.7) × 10^8	30 ± 2
	TC-AChE[d]	4100 ± 800	(1.0 ± 0.1) × 10^8	*e*

[a] Reaction temperature was 25.0 ± 0.1 °C. Oxy ester reactions were run in 0.3 mM *p*-nitrophenol buffers, pH 7.2–7.6, that contained 0.25 M NaCl, 0.1–1 mM TX100, and 1–2% MeCN (v/v). Thioester reactions were run in 0.05 M sodium phosphate buffers, pH 7.1–7.2 (ionic strength = 0.25 with NaCl), that contained 0.3–0.9 mM DTNB. For EE-AChE-catalyzed hydrolysis of ATCh (Y = S, X = N^+Me_3), reaction mixtures also contained 0.011 mM TX100 and 1% MeCN (v/v). [b] Substrate structures are displayed in Chart 1. [c] Because initial velocities could not be measured at sufficiently high substrate concentrations, these parameters could not be determined. [d] Measured at the University of California—San Diego. Reaction conditions were as described in footnote *a*, save that the pH was 7.0. [e] Not measured.

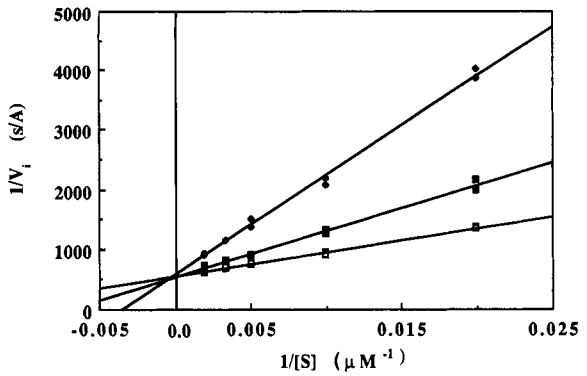

FIGURE 2: Mixed inhibition of TC-AChE-catalyzed hydrolysis of ATCh by *m*-ethyltrifluoroacetophenone, **3**. Reactions were run at 25.0 ± 0.1 °C in 0.05 M sodium phosphate buffer, pH 7.26, that contained 0.12 M NaCl, 0.3 mM DTNB, 1% (v/v) MeCN, 35 pM TC-AChE, and the various substrate concentrations plotted as reciprocals. The displayed linear fits were constructed from Michaelis–Menten parameters that were calculated by fitting (V_i, [S]) data to eq 2.

an observation that is consistent with the following two-state inhibition mechanism:

$$E + I_k \underset{k_{off}}{\overset{k_{on}}{\rightleftarrows}} E\text{–}I_k$$

I_k represents the free ketone form of the inhibitor. Equation 9 describes the dependence of the observed first-order rate constant on [I] for this mechanism:

$$k = k_{on}'[I] + k_{off} \tag{9}$$

From the slope and intercept of eq 9, $k_{on} = k_{on}'(1 + [S]/K_m)(1 + K_{hyd})$ and k_{off}, respectively, were determined. The equation for k_{on} corrects the observed k_{on}' for the facts that part of the enzyme is bound by substrate and only the free ketone inhibits. Moreover, $K_i = k_{off}/k_{on}$. Dissociation and rate constants so determined for time-dependent trifluoro ketone inhibitors are contained in Table 3. K_i values were also determined by fitting v_{ss} data to eq 6 (Wentworth, 1965), and are contained in Table 3. Comparisons of k_{on} values for charged and uncharged inhibitors are of some interest. For TC-AChE the *m*-Me_3N^+ inhibitor binds ~20 times faster than do inhibitors that have *m*-*i*Pr or *m*-*t*Bu substituents, while for EE-AChE a similar comparision indicates that the charged inhibitor binds 30–70 times faster. The markedly more facile binding of the quaternary ammonio inhibitor than of inhibitors that possess *m*-alkyl functions is a likely signature of the electrostatic field of AChE (Ripoll *et al.*, 1993; Tan *et al.*, 1993). These interesting and important comparisons will be revisited in the Discussion section.

As Figure 4 shows, the time-dependent inhibition of EE-AChE by *m*-(*N*,*N*-dimethylamino)trifluoroacetophenone (compound **8**) is marked by a nonlinear dependence of k_{obs} on [I]. This observation is consistent with a mechanism that involves successive complexes, an initial complex, E·I_k, and a subsequent, more tightly bound form:

$$E + I_k \underset{k_2}{\overset{k_1}{\rightleftarrows}} E\cdot I_k \underset{k_4}{\overset{k_3}{\rightleftarrows}} E\text{–}I_k$$

Putative structural assignments for E·I_k and E–I_k will be proffered in the Discussion. If one assumes that rapid, reversible formation of E·I_k precedes slow isomerization to E–I_k (i.e., that $k_3 \ll k_2$), then the requisite expression for time-dependent AChE inhibition is the following, in which v and v_0 are enzyme activities at times t and 0, respectively:

$$v = \frac{v_0}{1 + [I]/K_{21}'}\left|\frac{k_4}{k_3' + k_4} + \frac{k_3'}{k_3' + k_4}e^{-k_{obs}t}\right| \tag{10}$$

Equations 11–13 provide additional definitions of terms in eq 10:

$$k_{obs} = k_4 + \frac{k_3[I]}{K_{21}' + [I]} \tag{11}$$

$$k_3' = \frac{k_3[I]}{[I] + K_{21}'} \tag{12}$$

$$K_{21}' = K_{21}(1 + K_{hyd})(1 + [S]/K_m), \text{ where } K_{21} = k_2/k_1 \tag{13}$$

The dependence of k_{obs} on [I] in Figure 4 was fit to eq 11, and the resulting values of K_{21} and k_3 are given in Table 4. When $t = 0$, eq 10 reduces to an expression that is equivalent to eq 3, with $K_i^{app} = K_{21}'$. Hence, for TC-AChE, initial velocities of inhibition time courses were measured and fit to eq 3; the resulting value of K_{21} is given in Table 4. Finally, at long reaction times $e^{-k_{obs}t}$ goes to zero and eq 10 reduces to eq 14:

$$v_{ss} = \frac{v_0 K_4'}{[I] + K_4'}, \text{ where } K_4' = \frac{K_{21}'}{1 + k_3/k_4} \tag{14}$$

K_4 is calculated by dividing K_4' by $(1 + K_{hyd})(1 + [S]/K_m)$. Data are fit in Figure 4B to eq 14, and the resulting values are given in Table 4.

DISCUSSION

Inhibition Mechanisms. The results described herein indicate that, within a structurally congeneric series of trifluoro ketone inhibitors of AChE, three types of inhibition kinetics are observed. Compounds that possess the diminutive *meta* substituents H, Me, Et, CF_3, NH_2, and NO_2 are rapid reversible inhibitors. These compounds have dissociation constants, or K_i' values, in the micromolar range, which on adjustment for ketone hydration give K_i values in the nanomolar range. This observation is consistent with previous reports of AChE inhibition by ketones (Allen & Abeles, 1989; Brodbeck *et al.*, 1979; Dafforn *et al.*, 1976, 1982; Gelb *et al.*, 1985; Linderman *et al.*, 1988). As the size and polarizability of the *meta* substituent are increased, time-dependent inhibition is observed. For compounds with isopropyl, *tert*-butyl, and Me_3N^+ substituents the kinetics of inhibition are consistent with the accumulation on the enzyme of a single EI complex. However, when the *meta* substituent is Me_2N, the inhibition kinetics indicate that two EI complexes are formed. It is possible that the weaker complex is not on the pathway to formation of the tighter complex; i.e., parallel inhibition pathways are manifested. However, an alternate explanation, and one that represents greater mechanistic economy, is that serial EI complexes are being detected. The final, tighter complex is probably a hemiketal analog of the acylation transition state, as discussed below. Assignment of the weaker complex is the subject of more adventurous speculation, however. An attractive possibility is that the weaker complex is that in which the free ketone is bound at the active site, but in which S200 has not yet added to the carbonyl function of the inhibitor. In this case the rate constants k_3 and k_4 are those for the on-enzyme equilibrium formation of the hemiketal.

Table 2: Inhibition Constants for Rapid Trifluoro Ketone Inhibitors of Acetylcholinesterases[a]

inhibitor	K_{hyd}[b]	enzyme	K_i^E, nM[c]	K_i^{ES}, μM[d]	β[d]
$PhCOCF_3$ (1)	500	EE-AChE	20 ± 3		
		TC-AChE	63 ± 7		
		TC-AChE	90 ± 10[d]	1.81 ± 0.04	0.88 ± 0.01
m-$MeC_6H_4COCF_3$ (2)	500	EE-AChE	1.9 ± 0.3		
		TC-AChE	2.4 ± 0.3		
		TC-AChE	2.9 ± 0.3[d]	2 ± 2	0.72 ± 0.08
m-$EtC_6H_4COCF_3$ (3)	330	EE-AChE	0.22 ± 0.03		
		TC-AChE	0.40 ± 0.05		
		TC-AChE	0.48 ± 0.05[d]	2.5 ± 0.2	0
m-$CF_3C_6H_4COCF_3$ (6)	12 500	EE-AChE	0.43 ± 0.05		
		TC-AChE	0.40 ± 0.05		
		TC-AChE	0.58 ± 0.06[d]	103 ± 9	0
m-$H_2NC_6H_4COCF_3$ (7)	160	EE-AChE	36 ± 4		
		TC-AChE	160 ± 20		
			90 ± 10		
		TC-AChE	140 ± 20[d]	10 ± 3	0.78 ± 0.02
m-$O_2NC_6H_4COCF_3$ (10)	15 600	TC-AChE	3.2 ± 0.5[d]	400 ± 100	0.49 ± 0.05

[a] Inhibition assays were conducted in 0.05 M sodium phosphate buffers, pH 7.2 (ionic strength = 0.25 with NaCl), that contained 0.2–0.5 mM DTNB, 1% MeCN (v/v), 0.02–0.03 mM TX100, 30–60 pM EE-AChE or 35 pM TC-AChE, and various concentrations of ATCh. [b] Hydration equilibrium constants are single determinations; estimated uncertainty is ± 10%. [c] Except where indicated, K_i^{app} values were determined by fitting (v_i, [I]) data obtained at a single substrate concentration to eq 3; K_i^E was calculated from K_i^{app} according to eqs 7 and 8. Error limits are standard errors, propagated from the least-squares errors in K_i^{app} and K_m and the estimated uncertainty of K_{hyd}. [d] V_{app} and K_m^{app} were determined by fitting (v, [S]) data, obtained at several inhibitor concentrations, to the Michaelis–Menten equation (eq 2). K_i^E and K_i^{ES} were then calculated by nonlinear least-squares fits (Wentworth, 1965) to the following equations: $V_{app} = V(\beta[I] + K_i^{ES})/([I] + K_i^{ES})$; $V_{app}/K_m^{app} = (V/K)K_i^E(1 + K_{hyd})/([I] + K_i^E(1 + K_{hyd}))$. The parameter β is a measure of the residual catalytic turnover of the ESI complex.

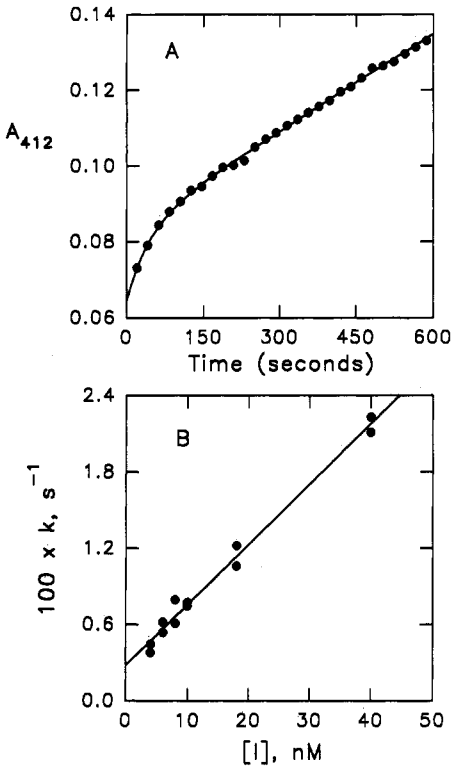

FIGURE 3: Time-dependent inhibition of TC-AChE-catalyzed hydrolysis of ATCh by *m*-isopropyltrifluoroacetophenone, **4**. (A) Biphasic time course for inhibition by **4**. The reaction was run at 25.0 ± 0.1 °C in 0.05 M sodium phosphate buffer, pH 7.26, that contained 0.12 M NaCl, 0.05 mM ATCh (=K_m/1.4), 0.15 mM DTNB, 1% (v/v) MeCN, 40 nM **4**, and 35 pM TC-AChE. The solid line is a nonlinear least-squares fit to eq 4; the parameters of the fit are A_0 = 0.0644 ● 0.0002, k = 0.0223 ± 0.0004 s^{-1}, v_{ss} = (8.56 ± 0.02) × 10^{-5} A s^{-1}, and v_0 = (5.1 ± 0.1) × 10^{-4} A s^{-1}. (B) Linear dependence of k on [I] for inhibition by **4**. The solid line is a linear least-squares fit to eq 9; the parameters of the fit are k_{on}' = (4.7 ± 0.2) × 10^5 M^{-1} s^{-1} and k_{off} = (2.9 ± 0.3) × 10^{-3} s^{-1}.

The most straightforward assignment for the mode of binding to AChE of trifluoro ketones is that S200 of the active site reversibly forms a covalent hemiketal adduct with the carbonyl carbon. This inhibition mechanism is supported by ^{19}F NMR characterization of the interaction of 3-(octylthio)-1,1,1-trifluoropropan-2-one with EE-AChE (Linderman *et al.*, 1988). The bound inhibitor is marked by a broad resonance that is distinct from those of the keto and hydrated forms in both chemical shifts and line widths. Moreover, analogs of trifluoro ketones in which the carbonyl is reduced to the corresponding racemic secondary alcohols are poor AChE inhibitors (Allen & Abeles, 1989; Nair *et al.*, 1993). Brodbeck *et al.* (1979) reported that 1,1,1-trifluoropropan-2-one inhibits EE-AChE with an observed K_i of 0.1 mM, but the sterically similar 1,1,1,3,3,3-hexafluoropropan-2-one did not inhibit. The latter compound is irreversibly hydrated in aqueous solution, and hence no free ketone is available to inhibit AChE.

Quantitative Structure–Activity Relationships (QSARs). The aryl trifluoro ketones described herein are rigid analogs of the acylation transition state, as supported by the following observations: (1) In the acylation transition state AChE binds the extended substrate conformation in which the quaternary nitrogen and the ester function are in an *anti* relationship. This conformation is supported by molecular modeling of tetrahedral intermediates in ACh (Sussman *et al.*, 1991) and ATCh (Selwood *et al.*, 1993) hydrolyses. Also, Smissman and co-workers found that conformationally rigid analogs of ACh in which the quaternary nitrogen and the ester function are *gauche* are AChE inhibitors, while those in which the groups are *anti* are substrates (Smissman *et al.*, 1966; Smissman & Parker, 1973; Stephen *et al.*, 1972). In the aryl trifluoro ketones the substituent X and the ketone function are constrained in an orientation that mimics the *anti* conformation of substrates. (2) In molecular models of ACh and the inhibitor in which X = Me_3N^+, the quaternary nitrogen to carbonyl carbon distances were nearly identical, 4.97 and 5.04 Å, respectively.

That the trifluoro ketones are functioning as transition-state analogs is suggested by the Thompson plots (Allen & Abeles, 1989; Bartlett & Marlowe, 1983; Thompson, 1973) in Figure 5, which show linear correlations of $\log(k_{cat}/K_m)$ for acetate ester substrates and pK_i of inhibitors for both TC-AChE and EE-AChE. Such correlations indicate that

Table 3: Inhibition and Rate Constants for Time-Dependent Trifluoro Ketone Inhibitors of Acetylcholinesterase[a]

inhibitor	K_{hyd}[b]	enzyme	K_i,[c] fM	k_{on}, M^{-1} s^{-1}	k_{off},[d] s^{-1}
m-*i*Pr (**4**)	390	TC-AChE	8500 ± 900	(3.2 ± 0.4) × 10^8	(2.9 ± 0.3) × 10^{-3}
		EE-AChE	4700 ± 600	(2.4 ± 0.4) × 10^8	(1.1 ± 0.2) × 10^{-3}
m-*t*Bu (**5**)	500	TC-AChE	3600 ± 400	(3.1 ● 0.4) × 10^8	(8 ± 4) × 10^{-4}
		EE-AChE	1900 ± 200	(1.2 ± 0.2) × 10^8	(2.6 ± 0.6) × 10^{-4}
m-Me_3N^+ (**9**)	62 500	TC-AChE	15 ± 5	(6 ± 1) × 10^9	(1.0 ± 0.3) × 10^{-4}
		EE-AChE	1.3 ± 0.4	(8 ± 1) × 10^9	(1.0 ± 0.2) × 10^{-5}

[a] Inhibition assays were conducted as described in footnote *a* of Table 2. Data for compound **9** were taken from Nair *et al.* (1993) or calculated from data contained therein. [b] Hydration equilibrium constants are single determinations, save that for **9**, which was measured twice; estimated uncertainty is ±10%. [c] For inhibitors **4** and **5** K_i values were determined by fitting (v_{ss}, [I]) data to eq 6. [d] For inhibitors **4** and **5** k_{off} values were determined as intercepts of linear fits of data to eq 9, save for inhibition of EE-AChE by **4**, where $k_{off} = K_i k_{on}$.

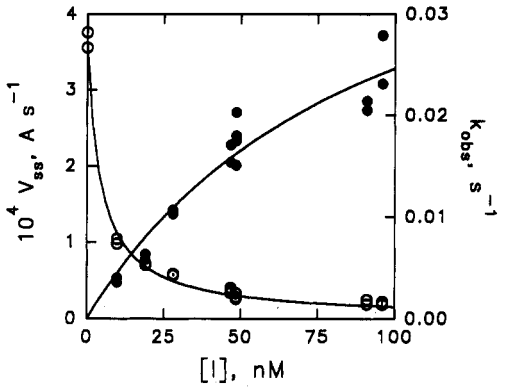

FIGURE 4: Time-dependent inhibition of EE-AChE-catalyzed hydrolysis of ATCh by *m*-(*N*,*N*-dimethylamino)trifluoroacetophenone, **8**. Reactions were run at 25.0 ± 0.1 °C in 0.05 M sodium phosphate buffer, pH 7.31 (ionic strength = 0.2 with NaCl), that contained 0.038 mM ATCh (=K_m/3.7), 0.3 mM DTNB, 20 pM EE-AChE, and the various indicated concentrations of **8**. Closed circles show the dependence of k_{obs} on [I]. The corresponding solid line is a nonlinear least-squares fit (Wentworth, 1965) to eq 11 with k_4 set to 0; the parameters calculated from the fit are k_3 = 0.048 ± 0.009 s^{-1} and K_{21}' = 100 ± 30 nM. Open circles show the dependence of v_{ss} on [I]. The corresponding line is a nonlinear least-squares fit to eq 14; the parameters calculated from the fit are v_0 = 3.65 ± 0.08 A s^{-1} and K_4' = 4.3 ± 0.1 nM.

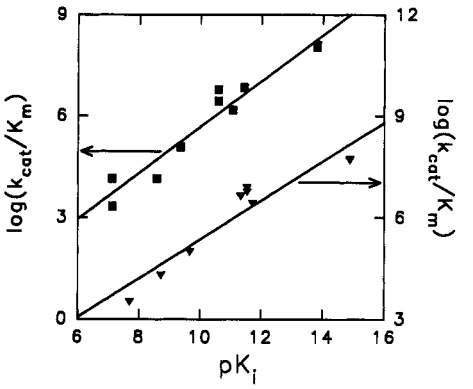

FIGURE 5: Thompson plots for inhibition of AChE by aryl trifluoro ketone transition-state analogs. Squares and triangles show data for TC-AChE and EE-AChE, respectively. The slopes of the respective plotted lines are 0.68 ± 0.06 and 0.57 ± 0.07.

Table 4: Inhibition and Rate Constants for Interaction of AChE with *m*-(*N*,*N*-Dimethylamino)trifluoroacetophenone, **8**[a]

enzyme	K_{21}, pM	K_4, pM	k_3, s^{-1}	k_4, s^{-1}
EE-AChE[b]	70 ± 20	3.1 ± 0.3	0.048 ± 0.009	(2.2 ± 0.8) × 10^{-3}
	110 ± 30	3.1 ± 0.3	0.07 ± 0.01	(1.9 ± 0.7) × 10^{-3}
	60 ± 30	3.7 ± 0.4	0.06 ± 0.02	(4 ± 2) × 10^{-3}
TC-AChE[c]	52 ± 8	25 ± 3		

[a] Inhibition assays were conducted as described in footnote *a* of Table 2. K_{hyd} for inhibitor **8** is 1100. [b] Because fits to eq 11 gave k_4 values that were negative and/or that had least-squares uncertainties of ~±100%, k_4 was set to 0 and fits to eq 11 were recalculated. K_4 values were calculated by nonlinear least-squares fits of v_{ss} versus [I] data to eq 14. Values of k_4 were calculated as follows: $k_4 = k_3/[(K_{21}'/K_4') - 1]$. [c] K_{21}' and K_4' were calculated by fitting data to eqs 3 and 14, respectively.

structural features that stabilize inhibitor complexes, in particular substituents that are large and polarizable, also stabilize chemical transition states[3] in the acylation stage of catalysis. However, the slopes of the plots are ~0.6, and hence the acylation transition state is not as sensitive to stabilizing interactions in the anionic site as the trifluoro ketone inhibitors. Trifluoro ketones bind in a manner that resembles the tetrahedral intermediate in the acylation stage of catalysis (Quinn, 1987). The chemical transition state lies structurally between the reactant state, in which the ester carbonyl is sp^2 hybridized, and the tetrahedral intermediate in which the carbonyl is sp^3 hybridized. Hence, substituents that improve interaction in the anionic locus specifically stabilize the tetrahedral intermediate, which by Hammond's postulate also leads to stabilization, though somewhat less, of the transition states that lead to and from the intermediate. Overall, substituent variation enhances inhibitor potency by ~10^7-fold and k_{cat}/K_m for substrate turnover by ~10^5-fold. These large ranges underscore the importance of molecular recognition in the anionic locus for AChE–ligand interactions. Moreover, the range for substrates represents a substantial fraction of the 10^{13}-fold catalytic acceleration wrought by AChE (Quinn, 1987), and therefore the structure–activity trends reported herein should shed light on the origins of the enzyme's catalytic power.

The active site of AChE consists of esteratic and anionic subsites that respectively effect covalent bond rearrangements and interact with the quaternary ammonium pole of substrates (Froede & Wilson, 1971; Quinn, 1987; Rosenberry, 1975; Sussman *et al.*, 1991). Various roles have been suggested for the amino acid constituents that comprise the anionic site. Hasan *et al.* (1980) found that k_{cat}/K_m correlated with partial molal volume of the alcohol leaving group for reactions catalyzed by EE-AChE, and hence claimed that there was no anionic site but rather that a hydrophobic trimethyl binding site accommodates the quaternary ammonium pole of ACh. As Figure 6 shows, there is a good linear correlation for TC-AChE between pK_i for aryl trifluoro ketone inhibitors and the Hansch hydrophobicity parameter (Hansch & Leo, 1989) when the *meta* substituents are H, alkyl, and CF_3. However, the correlation fails miserably when the *meta* substituents contain nitrogen atoms. The *m*-NH_2 and *m*-NMe_2 inhibitors are 300-fold and 1000-fold more potent, respectively, than predicted by the linear correlation, while the inhibitor that contains Me_3N^+ (π = –5.96) is *20* orders of magnitude more potent than predicted! EE-AChE also gives a linear correlation of pK_i and π when the *meta* substituents are H, alkyl, and

[3] The term "chemical transition state" refers to the transition state of an elementary step in which covalent bond rearrangements are occurring.

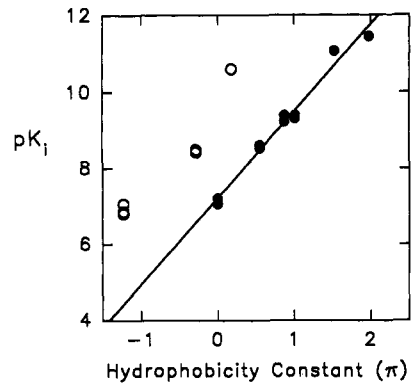

FIGURE 6: Plot of pK_i versus substituent hydrophobicity parameter for inhibition of TC-AChE by *m*-$XC_6H_4COCF_3$. Plotted from left to right as solid circles are data for inhibitors that have substituents X = H, Me, CF_3, Et, *i*Pr, and *t*Bu. Plotted from left to right as open circles are data for inhibitors whose substituents are NH_2, NO_2, and NMe_2.

CF_3, but the observations for the NH_2, NMe_2, and Me_3N^+ inhibitors deviate from the correlation yet more than those shown in Figure 6 for TC-AChE. Clearly, the hydrophobic effect does not provide an adequate accounting of molecular recognition in the anionic site, particularly when the inhibitor or substrate contains the physiologically relevant quaternary ammonio group.

Substituent π values are based on octanol/water partition coefficients of substituted benzenes (Hansch & Leo, 1989). The slope of the plot in Figure 6, $m = 2.3 \pm 0.1$, indicates that the substituent effect on inhibitor partitioning into the AChE active site is much greater than that in the reference system. For EE-AChE the corresponding value is $m = 2.2 \pm 0.2$. These high sensitivities to substituent variation again indicate that hydrophobic effects are not sufficient to characterize molecular recognition in the anionic locus.

What, then, is the function of the constituents of the anionic site, Y130, F330, and in particular W84? And why does substituent hydrophobicity work well for most but not for all inhibitors? The three-dimensional correlation for TC-AChE in Figure 7A answers these questions. In this figure pK_i values are correlated with σ_m and molar refractivity, MR, of substituents according to the following equation:

$$pK_i = m\mathrm{MR} + \rho\sigma_m + c \qquad (15)$$

The data in Figure 7A were fit to this equation by multiple linear regression, and the resulting slopes along the MR and σ_m axes are $m = 0.28 \pm 0.03$ and $\rho = 1.3 \pm 0.5$. A similar correlation for EE-AChE gives $m = 0.28 \pm 0.02$ and $\rho = 2.1 \pm 0.5$. The correlations with σ_m are similar to that between K_{hyd}, the hydration equilibrium constant of the inhibitors, and σ_m:

$$\log(K_{hyd}) = (2.2 \pm 0.2)\sigma_m + 2.85 \pm 0.09 \qquad (16)$$

This similarity is not suprising, since a component of the binding of fluoro ketones to the AChE active site is addition of an oxygen nucleophile, the γO of S200, to the carbonyl carbon of the inhibitor. This process is modeled by the equilibrium hydration of the fluoro ketones, which also involves interaction with an oxygen nucleophile.

Figure 7B shows a linear correlation of $pK_i - \rho\sigma_m$ versus MR, constructed by rearranging eq 15. The quantitative contributions of all substituents are well modeled by this correlation. MR is a measure of the ability of a functional group or molecule to be involved in London dispersion

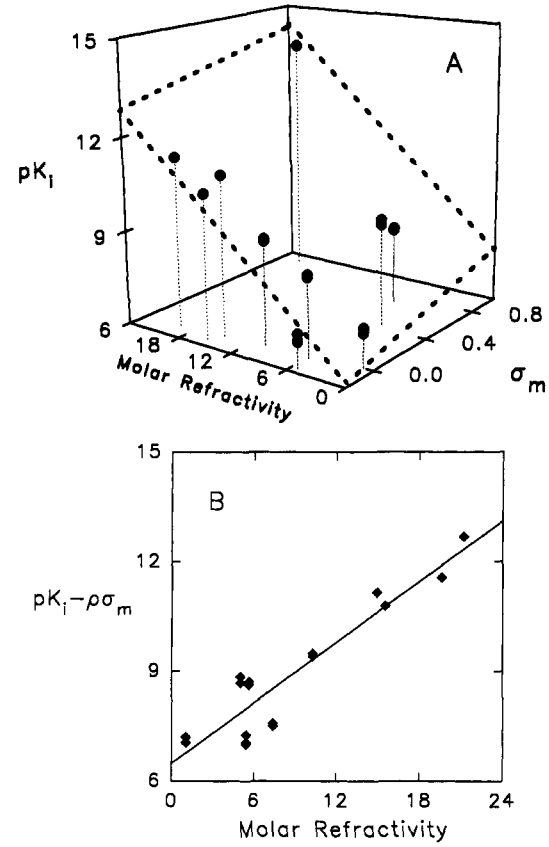

FIGURE 7: QSAR for inhibition of TC-AChE by *meta*-substituted aryl trifluoro ketones. (A) Three-dimensional plot of pK_i versus MR and σ_m values of inhibitor substituents. Substituent constants for the ten inhibitors are as follows (substituent, σ_m, MR): H, 0, 1.03; Me, −0.07, 5.65; Et, −0.07, 10.3; *i*Pr, −0.07, 14.96; *t*Bu, −0.10, 19.62; CF_3, 0.43, 5.02; NO_2, 0.71, 7.36; NH_2, −0.16, 5.42; NMe_2, −0.15, 15.55; Me_3N^+, 0.88, 21.2. The data were fit to eq 15, and the resulting gradients along the MR and σ_m axes are 0.28 ± 0.03 and 1.3 ± 0.5, respectively. The heavy dashed line shows the orientation of the least-squares best-fit plane, while the light dashed lines locate each point in the (MR, σ_m) plane. (B) Subcorrelation of inhibitor potency versus MR, plotted according to $pK_i - \rho\sigma_m = m\mathrm{MR} + c$. Plotted from left to right are data for inhibitors whose substituents are H, CF_3, NH_2, Me, NO_2, Et, *i*Pr, NMe_2, *t*Bu, and Me_3N^+.

interactions with a target site or molecule (Hansch & Leo, 1989). The energy of a London dispersion interaction between two atoms, a and b, is given by eq 17 (Pauling & Pressman, 1945; Hansch & Leo, 1989):

$$E = -\frac{3\alpha_a\alpha_b}{2r^6}\frac{I_aI_b}{I_a + I_b} \qquad (17)$$

Dispersion forces depend on r^{-6} and thus are short-range, and they increase as the polarizabilities α and the ionization potentials I of the interacting pair increase. The relationship between MR and the energy of a dispersion interaction is given by the following:

$$\mathrm{MR} = 4\pi N\alpha/3 \qquad (18)$$

Equations 17 and 18 show that as MR, and thus α, increases, the strength of the corresponding dispersion interaction increases. MR of a molecule or molecular substituent is characterized experimentally by using the Lorentz–Lorenz equation (Hansch & Leo, 1989):

$$\mathrm{MR} = \frac{n^2 - 1}{n^2 + 2}\frac{\mathrm{MW}}{d} \qquad (19)$$

MR thus depends on the refractive index, n, and MW/d, the molecular or substituent volume. One can see from eq 19 why Hasan *et al.* (1980) mistakenly labeled the anionic locus a "hydrophobic trimethyl binding site". Both the hydrophobic effect and London dispersion interactions increase as the surface areas, and hence the molecular or partial molal volumes, increase. Because of this and because there is usually very little variation in the refractive index term in eq 19 for a variety of organic species, the experimental vectors MR and π are usually collinear. In the study detailed herein, this collinearity was broken by the nitrogen-containing *meta* substituents, particularly Me_2N and Me_3N^+ (cf. Figure 7), which have high MR and low π values.

The excellent correlation with MR for all substituents in Figure 7B establishes the nature of molecular recognition effected by the aromatic constituents of the anionic locus. London dispersion interactions are maximal for substituents such as *t*Bu, *i*Pr, and Me_3N^+ that are polarizable and that have high surface areas. The aromatic amino acid constituents of the anionic locus (Y130, W84, and F330) in turn provide relatively loosely bound and hence polarizable π electron density that is easily distorted when the short-range, induced dispersion interaction is realized. In addition, of the aromatic amino acids, W84 is best suited to participate in dispersion interactions, since delocalization of the indole nitrogen lone pair increases the electron density and partial negative charge of the fused-ring aromatic system. This is reflected in the fact that the indole side chain of W has the highest MR of amino acid side chains (Hansch & Leo, 1989).

The results described herein contrast with certain ideas in the literature. One idea is that aromatic residues, in particular W84, provide an anionic site for interaction with the quaternary ammonio function of choline substrates (Ordentlich *et al.*, 1993). Figure 7B shows that the charged Me_3N^+ and uncharged alkyl substituents follow the same MR correlation, the linearity of which establishes that all substituents occupy a common locus on AChE. One certainly hesitates to suggest that W84 comprises an anionic site for any alkyl substituent. Another idea is that charged and uncharged substrates occupy different loci on AChE (Ordentlich *et al.*, 1993). If this were so, both the MR correlation of Figure 7B and the Thompson plots of Figure 5 would be nonlinear.

It is noteworthy that charge does not confer a particularly great advantage on the *m*-Me_3N^+ trifluoro ketone for interaction in the anionic locus. One can calculate from eq 15 that the inductive effect of *m*-Me_3N^+ on the equilibrium addition of S200 to the ketone carbonyl accounts for ~20-fold of the 240-fold tighter binding versus *m*-Me_3C. The remaining ~12-fold contribution is accommodated by the higher MR value of *m*-Me_3N^+ than of *m*-Me_3C, as the correlation in Figure 7B indicates. Moreover, the linear Thompson plots of Figure 5 suggest that the quaternary ammonium substituent of the physiological substrate ACh and the biomimetic substrate ATCh has a similar, though quantitatively smaller, electronic effect on chemical transition states in the acylation stage of catalysis. Therefore, the catalytic machinery of AChE has evolved two ways to utilize interactions with the quaternary ammonium function to effect rate acceleration of ACh hydrolysis. The aromatic amino acids of the anionic locus, and in particular W84, provide the sites for dispersion interactions that probably stabilize all EI complexes in the acylation stage of catalysis. Albery and Knowles refer to this mode of rate enhancement as "catalysis by uniform binding" (Albery & Knowles, 1976; Knowles & Albery, 1977). The esteratic locus, and in particular S200, responds to the electronic inductive effect of Me_3N^+ by stabilizing the tetrahedral intermediate, which by a Hammond effect produces a proportionate stabilization of the transition states leading to and from the intermediate. This mode of rate acceleration is referred to as catalysis by "differential binding" (Albery & Knowles, 1976; Knowles & Albery, 1977).

Ligand Trafficking in the Active Site Gorge: Electrostatic Steering or Aromatic Guidance? For time-dependent inhibitors the binding rate constants, k_{on}, fall cleanly into two numerical classes that depend on the structure of the *meta* substituent (cf. Table 3). When the substituent is *t*Bu or *i*Pr, k_{on} is $\sim 2 \times 10^8$ M^{-1} s^{-1}, which is similar to the estimate of Eigen and Hammes (1963) for the binding of a neutral ligand with a globular macromolecule. On the other hand, when the *meta* substituent is Me_3N^+, k_{on} is $\sim 7 \times 10^9$ M^{-1} s^{-1}. Interestingly, the ratio of k_{on} values for charged and uncharged aryl trifluoro ketone inhibitors is closely matched by the ratio of k_{cat}/K_m values for charged and uncharged substrates. From data in Table 1 one calculates k_{cat}/K_m ratios for ACh and 3,3-dimethylbutyl acetate of 20 for EE-AChE and 7–24 for TC-AChE. Hasan *et al.* (1980) reported a 40-fold ratio for the same substrates. There is ample evidence that k_{cat}/K_m of AChE-catalyzed hydrolyses of ACh and ATCh are diffusion controlled (Bazelyansky *et al.*, 1986; Hasinoff, 1982; Quinn, 1987). The similar quantitative effects of charge on inhibitor binding and substrate hydrolysis suggest that k_{cat}/K_m for turnover of 3,3-dimethylbutyl acetate is diffusion controlled as well.

The large k_{on} values for the trifluoro ketone inhibitor **9** (Nair *et al.*, 1993) are not without precedent. Nolte *et al.* (1980) measured a similar large value for *N*-methylacridinium binding at comparable ionic strength, $k_{on} = 6.4 \times 10^9$ M^{-1} s^{-1}. These high binding rate constants for quaternary ammonium aromatic ligands are certain indications of the accelerative effect of the electric field of AChE on ligand binding (Ripoll *et al.*, 1993; Tan *et al.*, 1993), which Tan *et al.* call "electrostatic steering". Electrostatic interactions are long range (i.e., they depend on r^{-2}), and hence it is enlightening but not too surprising that AChE has evolved an electrostatic guidance mechanism.

Sussman *et al.* (1991) noted that an unusually high fraction, ~40%, of the surface of the active site gorge of AChE comes from aromatic amino acids and suggested that "aromatic guidance" plays a role in the high rate of quaternary ammonio ligand binding. The QSAR results described herein suggest an alternate role for aromatic amino acids. The dispersion forces manifested in complexes with ligands and substrates are short-range forces (i.e., they depend on r^{-6}; cf. eq 17). Hence, these interactions stabilize ES complexes, including transition states, in the acylation stage of catalysis but dissipate rapidly with distance and thus do not impede product release sufficiently that it becomes kinetically significant. Thus, the high catalytic power of AChE results in part from a combination of transition-state stabilization by aromatic amino acids of the "anionic locus" and rapid ligand transport effected by the electrical field of the enzyme.

Alternate Ligand Binding Sites. Substrate inhibition constants, or K_{ss} values, have been measured for acetate and thioacetate esters that have substituents X = *t*Bu, NHMe, NMe_2, and Me_3N^+ (cf. Chart 1 and Table 1). There is no trend in K_{ss} as the molar refractivity or hydrophobicity of X varies. Rather, substrate inhibition is most effective when X = NMe_2, the substituent of intermediate size. Though a substrate inhibition binding site cannot be assigned from these

few observations, there are two loci that can be excluded. One is the W84/Y130/F330 locus. If substrate inhibition is caused by binding in this locus in the acylenzyme intermediate, for example, one would expect K_{ss} to correlate with MR. Another site that can be excluded is the Y70/Y121/W279 locus near the opening of the active site gorge. Again one expects that substrate binding in this locus would be marked by a correlation of K_{ss} with MR.

Mixed inhibition is noted for aryl trifluoro ketones that are rapid AChE inhibitors (cf. Figure 2 and Table 2). The nature of the V_{max} inhibition depends on the size of the *meta* substituent. When this substituent is small (i.e., H, Me, NH_2, NO_2), the ESI complex is leaky, as reflected by β values > 0.4. However, for the larger *meta* substituents CF_3 and Et the ESI complex does not turn over (i.e., $\beta = 0$). This association of ESI leakiness with substituent size suggests that the inhibitor binds in the active site gorge and, when the substituent is sufficiently large, blocks release of products from the enzyme. Again, the binding site is likely not that comprising Y70, Y121, and W279, since there is no correlation between pK_i^{ES} and MR.

Conclusions. The results described in this paper provide an important lesson in the establishment and interpretation of structure–function relationships for AChE catalysis. Without a proper appreciation of the role of amino acid residues in the native enzyme, it is easy to misunderstand the results of site-directed mutagenesis and other structural experiments. The function of aromatic residues of the anionic locus, and in particular W84, is to provide a polarizable surface for short-range dispersion interactions. In the expression of AChE catalytic power W84 functions neither as an anionic site nor as a hydrophobic site. Though the role of W84 in dispersion interactions was revealed by structural variation in inhibitors and substrates, this role can also be gleaned from modification of the structure of the enzyme. For example, if W84 is changed to A, one predicts the following effect on k_{cat}/K_m of ATCh turnover:

$$\log \frac{(k_{cat}/K_m)_{W84}}{(k_{cat}/K_m)_{A84}} = 0.5 \times 0.68 \times 0.28 \times (MR_W - MR_A) = 3.37 \quad (20)$$

The factor 0.5 accounts for the fact that the quaternary ammonium function of ATCh interacts with one of two faces of W; 0.28 is the MR sensitivity from eq 15; 0.68 is the slope of the Thompson plot of Figure 5; and MR_W and MR_A are the respective molar refractivities of the 3-indolyl and proton substituents at the β-carbons of W and A, i.e., 36.44 and 1.03 (Hansch & Leo, 1989). The k_{cat}/K_m ratio calculated from eq 20, 2350 (3.37 log units), is in substantial agreement with the observed 3100-fold effect (3.50 log units) for the W84A mutant of human AChE (Ordentlich *et al.*, 1993).

Dougherty and co-workers have characterized the interactions of quaternary ammonium and other cationic ligands with synthetic cyclophane hosts (Dougherty & Stauffer, 1990; Kearney *et al.*, 1993). They view the host as a mimic of biological ACh receptors and ascribe its affinity for quaternary ammonium ligands to the "cation–π interaction". The results described herein demonstrate that, at least for molecular recognition by AChE, cationic ligands are not particularly remarkable. The dispersion interactions that recognize the highly polarizable quaternary ammonium function also accommodate polarizable but electrically neutral functions. Though our view differs in detail with that of Dougherty and co-workers, we share a common perspective that aromatic residues are crucial for molecular recognition of the quaternary ammonium function, whether that recogntion functions in biological or biomimetic chemistry.

ACKNOWLEDGMENT

We thank Palmer Taylor, Daniel Vellom, Natalie Pickering, and Zoran Radic for helpful comments on various aspects of this work and all of the members of the Taylor research group for their hospitality during D.M.Q.'s sabbatical at UCSD. The technical assistance of Danny Power is gratefully acknowledged. We thank Israel Silman of the Weizmann Institute for providing purified *Torpedo californica* AChE and Ms. Lilly Toker for skillful preparation of the enzyme. Molecular modeling studies were conducted at the University of Iowa Image Analysis Facility.

REFERENCES

Albery, W. J., & Knowles, J. R. (1976) *Biochemistry 15*, 5631–5640.
Allen, K. N., & Abeles, R. H. (1989) *Biochemistry 28*, 8466–8473.
Bartlett, P. A., & Marlowe, C. (1983) *Biochemistry 22*, 4618–4624.
Bazelyansky, M., Robey, E., & Kirsch, J. F. (1986) *Biochemistry 25*, 125–130.
Brodbeck, U., Schweikert, K., Gentinetta, R., & Rottenberg, M. (1979) *Biochim. Biophys. Acta 567*, 357–369.
Carroll, R. T., & Emmerling, M. R. (1991) *Biochem. Biophys. Res. Commun. 181*, 858–862.
Cha, S. (1975) *Biochem. Pharmacol. 24*, 2177–2185.
Dafforn, A., Kerr, P., & Murray, R. R. (1976) *Biochem. Biophys. Res. Commun. 73*, 323–329.
Dafforn, A., Neenan, J. P., Ash, C. E., Betts, L., Finke, J. M., Garman, J. A., Rao, M., Walsh, K., & Williams, R. R. (1982) *Biochem. Biophys. Res. Commun. 104*, 597–602.
Dougherty, D. A., & Stauffer, D. A. (1990) *Science 250*, 1558–1560.
Eigen, M., & Hammes, G. G. (1963) *Adv. Enzymol. Relat. Subj. Biochem. 25*, 1–38.
Ellman, G. L., Courtney, K. D., Andres, V., Jr., & Featherstone, R. M. (1961) *Biochem. Pharmacol. 7*, 88–95.
Fersht, A. (1974) *Proc. R. Soc. London B187*, 397–407.
Froede, H. C., & Wilson, I. B. (1971) *Enzymes (3rd Ed.) 5*, 87–114.
Gelb, M. H., Svaren, J. P., & Abeles, R. H. (1985) *Biochemistry 24*, 1813–1817.
Hansch, C., & Leo, A. (1989) *Substituent Constants for Correlation Analysis in Chemistry and Biology*, John Wiley & Sons, New York.
Harel, M., Schalk, I., Ehret-Sabatier, L., Bouet, F., Goeldner, M., Hirth, C., Axelsen, P. H., Silman, I., & Sussman, J. L. (1993) *Proc. Natl. Acad. Sci. U.S.A. 90*, 9031–9035.
Hasan, F. B., Cohen, S. G., & Cohen, J. B. (1980) *J. Biol. Chem. 255*, 3898–3904.
Hasan, F. B., Elkind, J. L., Cohen, S. G., & Cohen, J. B. (1981) *J. Biol. Chem. 256*, 7781–7785.
Hasinoff, B. B. (1982) *Biochim. Biophys. Acta 704*, 52–58.
Kearney, P. C., Mizoue, L. S., Kumpf, R. A., Forman, J. E., McCurdy, A., & Dougherty, D. A. (1993) *J. Am. Chem. Soc. 115*, 9907–9919.
Klabunde, K. J., & Burton, D. J. (1970) *J. Org. Chem. 35*, 1711–1712.
Knowles, W. J., & Albery, W. J. (1977) *Acc. Chem. Res. 10*, 105–111.

Linderman, R. J., Leazer, J., Roe, R. M., Venkatesh, K., Selinsky, B. S., & London, R. E. (1988) *Pestic. Biochem. Physiol. 31*, 187–194.
Nair, H. K., & Quinn, D. M. (1993) *Bioorg. Med. Chem. Lett. 3*, 2619–2622.
Nair, H. K., Lee, K., & Quinn, D. M. (1993) *J. Am. Chem. Soc. 115*, 9939–9941.
Nolte, H.-J., Rosenberry, T. L., & Neumann, E. (1980) *Biochemistry 19*, 3705–3711.
Ordentlich, A., Barak, D., Kronman, C., Flashner, Y., Leitner, M., Segall, Y., Ariel, N., Cohen, S., Velan, B., & Shafferman, A. (1993) *J. Biol. Chem. 268*, 17083–17095.
Pauling, L. (1948) *Am. Sci. 36*, 51–58.
Pauling, L., & Pressman, D. (1945) *J. Am. Chem. Soc. 67*, 1003–1012.
Quinn, D. M. (1987) *Chem. Rev. 87*, 955–979.
Radic, Z., Gibney, G., Kawamoto, S., MacPhee-Quigley, K., Bongiorno, C., & Taylor, P. (1992) *Biochemistry 31*, 9760–9767.
Ripoll, D. R., Faerman, C. H., Axelsen, P. H., Silman, I., & Sussman, J. L. (1993) *Proc. Natl. Acad. Sci. U.S.A. 90*, 5128–5132.
Rosenberry, T. L. (1975) *Adv. Enzymol. Relat. Areas Mol. Biol. 43*, 103–218.
Schlom, P. S., Gillespie, S., Selwood, T., Knuth, T. M., Seravalli, J., Nair, H. K., Doctor, B. P., & Quinn, D. M. (1994) *Chem. Res. Toxicol.* (submitted).
Schowen, R. L. (1978) in *Transition States of Biochemical Processes* (Gandour, R. D., & Schowen, R. L., Eds.) pp 77–114, Plenum Press, New York.
Segel, I. (1975) *Enzyme Kinetics*, pp 170–202, John Wiley & Sons, New York.
Selwood, T., Feaster, S. R., States, M. J., Pryor, A. N., & Quinn, D. M. (1993) *J. Am. Chem. Soc. 115*, 10477–10482.
Smissman, E. E., & Parker, G. R. (1973) *J. Med. Chem. 16*, 23–27.
Smissman, E. E., Nelson, W. L., LaPidus, J. B., & Day, J. L. (1966) *J. Med. Chem. 9*, 458–465.
Stephen, W. F., Smissman, E. E., Schowen, K. B., & Self, G. W. (1972) *J. Med. Chem. 15*, 241–243.
Stewart, R., & Vander Linden, R. (1960) *Can. J. Chem. 38*, 399–406.
Sussman, J. L., Harel, M., Frolow, F., Oefner, C., Goldman, A., Toker, L., & Silman, I. (1991) *Science 253*, 872–879.
Thompson, R. C. (1973) *Biochemistry 12*, 47–51.
Tan, R. C., Truong, T. N., McCammon, A., & Sussman, J. L. (1993) *Biochemistry 32*, 401–403.
Vellom, D., Radic, Z., Li, Y., Pickering, N. A., Camp, S., & Taylor, P. (1993) *Biochemistry 32*, 12–17.
Wentworth, W. E. (1965) *J. Chem. Educ. 42*, 96–103.